

Highly Selective Separation of Actinides from Lanthanides by Dithiophosphinic Acids: An in-Depth Investigation on Extraction, Complexation, and DFT Calculations

Zhipeng Wang,^{†,||} Ning Pu,^{‡,||} Yin Tian,^{*,§} Chao Xu,^{*,‡,Ⓜ} Fang Wang,[‡] Ying Liu,[†] Lirong Zhang,[†] Jing Chen,[‡] and Songdong Ding^{*,†,Ⓜ}

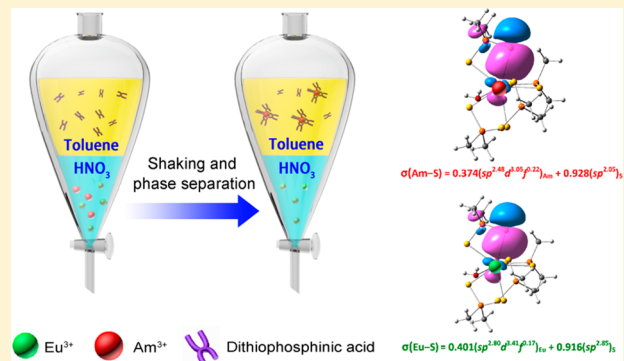
[†]College of Chemistry, Sichuan University, Chengdu 610064, P. R. China

[‡]Collaborative Innovation Center of Advanced Nuclear Energy Technology, Institute of Nuclear and New Energy Technology, Tsinghua University, Beijing 100084, P. R. China

[§]Key Laboratory of Radiation Physics and Technology, Ministry of Education, Institute of Nuclear Science and Technology, Sichuan University, Chengdu 610064, P. R. China

Supporting Information

ABSTRACT: To further reveal the extraction model for selective separation of trivalent actinides over lanthanides by dithiophosphinic acids (DPAHs), five representative DPAH ligands with different substituent groups have been synthesized, and their extraction and complexation behaviors toward Am³⁺/Eu³⁺ have been investigated both experimentally and theoretically. The introduction of electron-withdrawing group –CF₃ into DPAH ligands is beneficial to their extractability among the five ligands. Slope analyses show that both Am³⁺ and Eu³⁺ were extracted as tetra-associated species with DPAH ligands. In addition, the results obtained from luminescence spectroscopy, Raman spectroscopy, and ESI-MS suggest that all of the five DPAHs coordinate with Eu³⁺ mainly in the form of ML₃(HL)·(H₂O) (L represents deprotonated DPAH). Density functional theory (DFT) calculations on the thermodynamic parameters illustrate that the extractability of DPAHs is dominated by the deprotonation property of these ligands. Meanwhile, molecular orbital analysis indicates that the unoccupied valence orbitals of Am³⁺ display a stronger affinity to the sulfur lone electron pair than those of Eu³⁺, which should be one of the key factors contributing to the excellent selectivity of Am³⁺ over Eu³⁺ by DPAH ligands.



INTRODUCTION

The selective extraction of trivalent actinides (An³⁺) over trivalent lanthanides (Ln³⁺) is of great importance for the treatment of nuclear waste in the partitioning and transmutation strategy.¹ However, because An³⁺ and Ln³⁺ have similar chemical and physical properties, their separation from each other is a quite challenging task.^{2,3} According to the hard–soft acids–bases (HSAB) principle, An³⁺ is slightly softer as compared to Ln³⁺, thus it is feasible to use ligands containing soft N- or S-donor atoms to separate An³⁺ from Ln³⁺.^{4,5} Up to now, N-donor ligands such as 2,6-bis(5,6-dialkyl-1,2,4-triazin-3-yl)pyridines (BTPs), 6,6-bis(5,6-dialkyl-1,2,4-triazin-3-yl)-2,2-bipyridine (BTBPs), and 2,9-bis(1,2,4-triazin-3-yl)-1,10-phenanthroline (BTBPhens) have been widely studied for An³⁺/Ln³⁺ separation. Unfortunately, the poor irradiation stability as well as relatively poor extraction kinetics restricted their applications.^{6–9} Moreover, the An³⁺/Ln³⁺ separation factor ($SF_{An/Ln}$) of N-donor ligand is relatively small, causing difficulties in practical process design.¹⁰ In contrast, the S-donor ligands such as dithiophosphinic acids

(DPAHs) were found to show exceptional An³⁺/Ln³⁺ separation ability and thus have attracted great attentions.

Two representative DPAHs for An³⁺/Ln³⁺ separation are purified Cyanex 301 and (CIPh)₂PS₂H. The former is the purified product from a mixture containing a series of aliphatic organophosphorus including 75–83% R₂PS₂H, 5–8% R₃PS, 3–6% R₂PSOH, and ~2% unknown substances.¹¹ At pH 3.5–4.0, the purified Cyanex 301 (Figure 1) could afford an $SF_{Am/Eu}$ value up to 5900, and practical processes have been developed accordingly.^{12–15} The latter ligand (CIPh)₂PS₂H is an aromatic dithiophosphinic acid with better hydrolysis and radiolysis stability than Cyanex 301.¹⁶ Although numerous studies have been conducted to reveal the extraction and separation behavior of DPAHs toward An³⁺ and Ln³⁺, a few fundamental issues on the extraction system are still ambiguous. For example, previous studies suggested that different extraction mechanisms for An³⁺/Ln³⁺ separation by DPAHs may exist.

Received: June 12, 2018

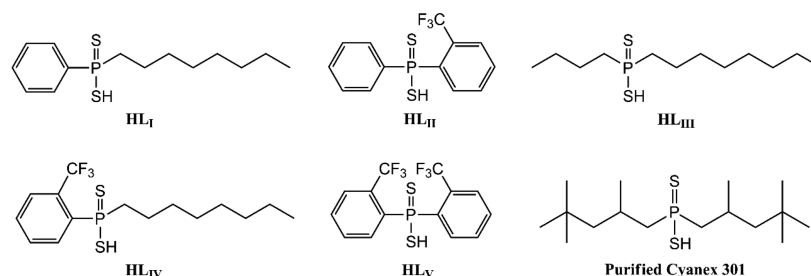
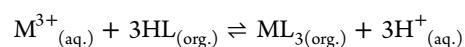
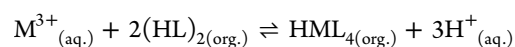


Figure 1. Chemical structures of DPAHs.

Both 1:4 and 1:3 metal:ligand extracted species have been reported:^{17–19}



where HL and M represent DPAH and metal ion, and the subscripts aq. and org. denote the aqueous and organic phases, respectively. Furthermore, there are also debates on the complexation mode. Using extended X-ray absorption fine structure spectroscopy (EXAFS), Tian et al. found that the compositions of the complexes of Am^{3+} and Ln^{3+} with DPAH are $HAmL_4$ and $HML_4(H_2O)$ ($M = La, Nd, Eu$), respectively. The excellent selectivity of DPAH toward Am^{3+} over Ln^{3+} may originate from the different coordination structures.^{20,21} In contrast, Jensen et al. suggested that both An^{3+} and Ln^{3+} form the same ML_3 ($M = Cm, Nd, Sm$) type complexes during extraction through visible absorption spectroscopy and EXAFS and proposed that the difference on the covalency degree leads to the selectivity toward An^{3+} .²² In addition, there are also different viewpoints in relevant theoretical calculations. Cao et al. pointed out that the Gibbs free energy of hydration for metal ions plays an important role for the high selectivity of Cyanex 301 to Am^{3+} .²³ Bhattacharyya et al. proposed that the higher affinity of DPAH to Am^{3+} than to Eu^{3+} is related to the stronger covalence in $Am-S$ bond as compared to that in $Eu-S$ bond.²⁴ Alternatively, Daly et al. suggested that the steric interactions of the substituent groups on DPAHs could impose great impact on the molecular symmetry and thus the complexation behavior with An^{3+} and Ln^{3+} .²⁵ Obviously, whether in experimental or in theoretical aspects, questions remain on the mechanism and complexation mode for the selective extraction of An^{3+} and Ln^{3+} by DPAHs. An in-depth investigation on these problems is necessary.

In the present work, by taking consideration of steric and electronic effects, five representative DPAHs (Figure 1) containing different alkyl and/or aryl substituent groups have been synthesized, and their extraction behaviors toward Am^{3+} and Eu^{3+} have been investigated using toluene as a diluent. Meanwhile, the complexation behaviors of Eu^{3+} with the five DPAHs have also been examined by luminescence spectroscopy, Raman spectroscopy, and electrospray ionization mass spectroscopy (ESI-MS). In addition, the extraction model and complexation mode of these DPAHs with Am^{3+} and Eu^{3+} have been studied by density functional theory (DFT) calculations.

EXPERIMENTAL SECTION

General. The stock solution of $^{241}Am^{3+}$ with radiochemical purity of 99.9% was supplied by China Institute of Atomic Energy. $Eu(NO_3)_3$ solution was prepared by dissolving Eu_2O_3 (99.99%, Aldrich, USA) in HNO_3 . Unless specifically noted, all the other

reagents in this work were of AR grade quality or higher and used as received. Tetramethylsilane (TMS) was the internal standard substance for 1H and ^{13}C NMR, and 85% H_3PO_4 solution was used as the external standard for ^{31}P NMR.

All NMR spectra were collected with a Varian Inova NMR spectrometer (1H : 400 MHz; ^{13}C : 100 MHz; ^{31}P : 240 MHz) (Bruker Inc., Switzerland). FT-IR and ESI-MS spectra were recorded on a Nicolet 6700 Fourier transform infrared spectrometer (Thermo Fisher Scientific Inc., USA) and Bruker Amazon SL spectrometer (Bruker Inc., Switzerland), respectively. The organic elemental analysis was performed on a Flash EA 1112 organic element analyzer (Thermo Fisher Scientific Inc., USA). The Lei Ci PHS-3C type pH meter (Shanghai Precision & Scientific Instrument Co. Ltd., China) was used for determining the pK_a values of DPAH compounds as well as the pH values of aqueous solutions. Luminescence titration was carried out on a F96Pro fluorescence spectrophotometer (Shanghai Leng Guang Technology Co. Ltd., China). Time-resolved fluorescence spectroscopy (TRFLS) was operated on a HORIBA TEMPRO-01 transient fluorescence spectrometer (HORIBA Ltd., Japan) with 370 nm as the excitation wavelength. Raman spectra were measured on LabRAM HR800 spectrometer (HORIBA Ltd., Japan) with 532 nm as the laser wavelength.

Synthesis. Ligands. All the DPAHs were synthesized with a halogenated organophosphorus compound as the initial reactant referring to the previous literature.²⁶ For (*n*-Oct)-(Ph)- PS_2H (**HL_I**) and (*o*- CF_3 Ph)-(Ph)- PS_2H (**HL_{II}**), PCl_2Ph was used as the starting material. Whereas for (*n*-Bu)-(*n*-Oct)- PS_2H (**HL_{III}**), (*n*-Oct)-(*o*- CF_3 Ph)- PS_2H (**HL_{IV}**), and (*o*- CF_3 Ph) $_2$ - PS_2H (**HL_V**), the reaction began with phosphorus trichloride. The halogenated organophosphorus compound reacted successively with the corresponding Grignard reagent, sulfur powder, and sodium hydrosulfide hydrate to give the crude product. Afterward, the crude was purified via recrystallization and acidification, resulting in the purified ligand with satisfying yields. The detailed procedures were summarized in the Supporting Information.

Eu^{3+} -DPAHs Complexes. Before preparation of the Eu^{3+} -DPAHs complexes, DPAHs were fully saponified by ammonium hydroxide. 0.2 mmol $Eu(NO_3)_3 \cdot 6H_2O$ dissolved in 10 mL EtOH/ H_2O (99/1%, v/v) was added dropwise to a solution of saponified ligands (1.2 mmol) in 20 mL EtOH/ H_2O (99/1%, v/v). The EtOH/ H_2O (99/1%, v/v) mixture was chosen as appropriate solvent for its good solubility to both ligands and metal salts. The mixed solution was vigorously stirred for 24 h and then washed with equal volumes of dichloromethane three times to remove the ammonium nitrate and unreacted ligands. Subsequently, the EtOH/ H_2O (99:1%, v/v) phase was collected through a separating funnel. After vacuum drying overnight, the oil-like Eu^{3+} -DPAHs complexes were obtained.

pH Titration. 0.75 mmol DPAH was dissolved in EtOH/ H_2O (99/1%, v/v) (50 mL) and then was titrated by 0.05 mol/L NaOH solution at 25.0 ± 0.5 °C. The pH values were recorded with a pH meter. Each ligand was titrated in triplicates. The pK_a values were determined through a linear regression method,^{27,28} and the purity of the examined compounds was also calculated.

Extraction. DPAHs were dissolved in toluene as the organic phase. The solution including trace amounts of $^{241}Am^{3+}$ and/or 200 ppm Eu^{3+} and 1.0 mol/L $NaNO_3$ was the aqueous phase.²⁴¹ Am^{3+} must be handled following strict regulations in radioactive glovebox

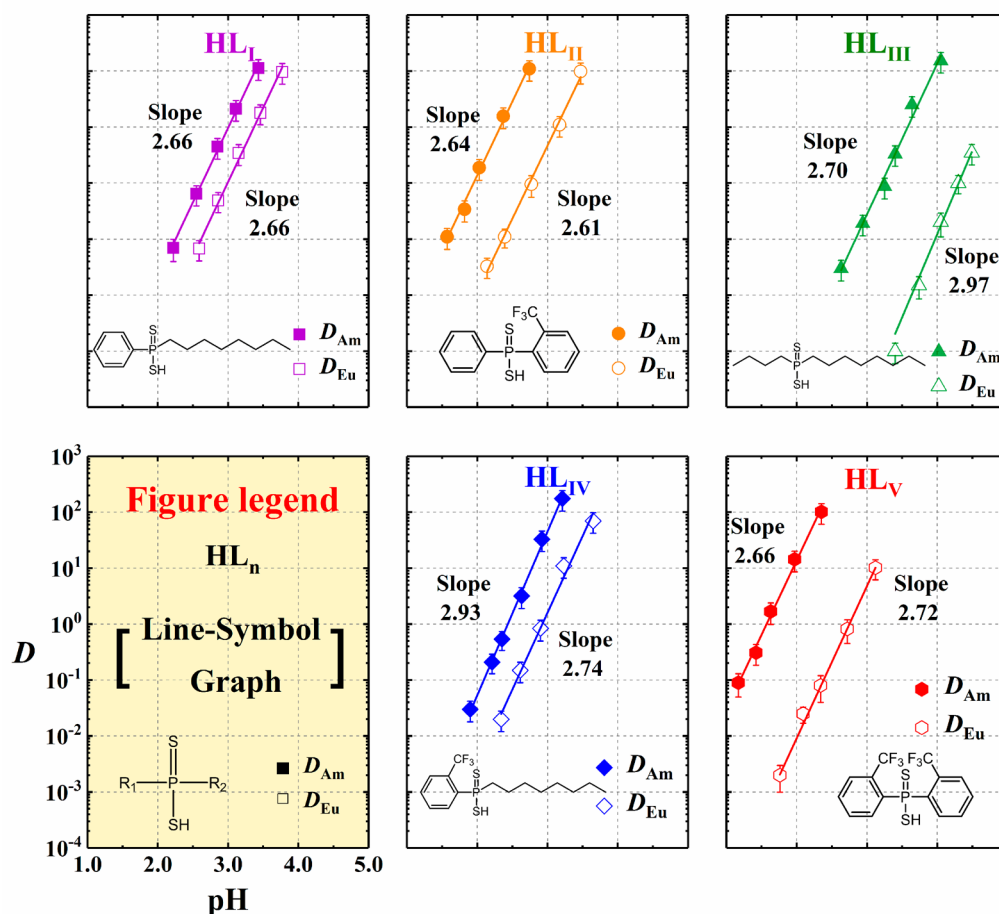


Figure 2. Influence of pH (equilibrium) on the distribution ratios of Am^{3+} and Eu^{3+} . Organic phase: 0.50 mol/L extractant in toluene. Aqueous phase: trace amount of $^{241}\text{Am}^{3+}$ and/or 200 ppm Eu^{3+} and 1.0 mol/L NaNO_3 in various HNO_3 solutions. Temperature: 25.0 ± 0.5 °C.

due to its high radioactivity and toxicity which may cause personal health hazards. The two phases were agitated for 0.5 h in a stoppered test tube with a phase ratio (O/A) of 1/1 at 25.0 ± 0.5 °C to achieve equilibrium. After centrifugal separation, the two phases were sampled, and the radiocounts of $^{241}\text{Am}^{3+}$ in both the organic phase and aqueous phase were measured by $\text{NaI}(\text{Tl})$ scintillation counter (China National Nuclear Inc., China). The concentration of Eu^{3+} in the aqueous phase was analyzed by inductively coupled plasma atomic emission spectrometer (ICP-AES, IRIS Advantage, Thermo Elemental Inc., USA), while that in the organic phase was calculated through mass balances by the difference between initial solution and the aqueous phase after extraction. The pH values of aqueous phases were finely adjusted by adding a micro amount of 1.0 mol/L HNO_3 or 1.0 mol/L NaOH . The distribution ratio (D) for $^{241}\text{Am}^{3+}$ or Eu^{3+} was defined as the ratio of metal-ion concentration in the organic phase ($[\text{M}]_{\text{org.}}$) to that in the aqueous phase ($[\text{M}]_{\text{aq.}}$), $D_{\text{M}} = [\text{M}]_{\text{org.}}/[\text{M}]_{\text{aq.}}$. The separation factor ($SF_{\text{Am/Eu}}$) was expressed as $SF_{\text{Am/Eu}} = D_{\text{Am}}/D_{\text{Eu}}$. Triplicate experiments were carried out to ensure that the uncertainty of extraction data was within 10% in the range of $10^{-2} < D < 10^2$.

Luminescence Titration. The luminescence titration was performed in 10 mm quartz cell. The initial solution was 1.0 mmol/L $\text{Eu}(\text{NO}_3)_3$ in $\text{EtOH}/\text{H}_2\text{O}$ (99/1v/v), and the titrant solution was 50 mmol/L DPAH in $\text{EtOH}/\text{H}_2\text{O}$. In each titration, appropriate aliquots of the titrant were added into the cell and stirred for 2 min, and then the emission spectra in the range of 550 to 750 at 0.1 nm intervals were collected with an excitation wavelength at 394 nm.

DFT Calculations. The ground-state electronic structures for all species were calculated by using Kohn–Sham DFT²⁹ with the Gaussian 09 code.³⁰ The hybrid exchange–correlation functionals M06-2X³¹ and B3LYP^{32,33} were employed in this work. In some cases, the Grimme’s D3-correction with Becke–Johnson damping [D3(BJ)]

was used to add London-dispersion correction.³⁴ The Stuttgart quasi-relativistic effective core potentials (RECPs) and their corresponding valence basis sets, using segmented contraction scheme, were used to describe the europium³⁵ and americium³⁶ atoms. The small-core RECPs represent 28 and 60 core electrons in europium and americium, respectively, while the remaining electrons were represented by the valence basis sets. The septet spin states were calculated for each Eu^{3+} and Am^{3+} species, because the high-spin ground-state configurations have been found to be consistent with experimental results.^{37,38} The double- ζ basis set 6-31+G(d) was used to describe hydrogen, carbon, oxygen, fluorine, sulfur, and phosphorus atoms.

All the geometries were fully optimized in aqueous medium by using the conductor-like polarized continuum model (CPCM)³⁹ with universal force field (UFF)⁴⁰ radii. The default fine grid (75, 302), having 75 radial shells and 302 angular points per shell, was used to evaluate the numerical integration accuracy. The harmonic vibrational frequencies were calculated after the geometry optimization to characterize the nature of each stationary point with all positive frequencies and to provide the thermodynamic quantities, such as the energy (E), enthalpy (H), and Gibbs free energy (G). In addition, the Wiberg bond indices (WBI)⁴¹ and natural atomic charges were analyzed on the basis of natural bond orbital (NBO)^{42,43} theory.

RESULTS AND DISCUSSION

pH Titration. According to previous results, the extractability of acidic DPAH ligands is closely related to their pK_a values.⁴⁴ In general, the ligand with higher acidity exhibits better extractability.⁴⁵ The pK_a values of the five DPAHs determined by pH titration are summarized in Table S1 in the

Supporting Information. These values are consistent with the predicted ones in a previous work.⁴⁶ As can be seen, the pK_a values increase in the following order: $HL_V < HL_{II} < HL_{IV} < HL_I < HL_{III} < \text{Cyanex 301}$. Obviously, the aromatic DPAH ligands have smaller pK_a values, which can be explained on the basis of the electronic property of the substituent groups. The electron-withdrawing groups such as Ph and *o*-CF₃Ph would result in lower electronic density on the S atom and thus lead to weaker protonation than those with electron-donating groups such as *n*-Oct and *n*-Bu. In addition, all of the five DPAHs show lower pK_a values than Cyanex 301, suggesting that they may be used for An^{3+}/Ln^{3+} separation under lower pH conditions than the latter (pH \sim 3.5).

Extraction. Preliminary experiments have shown that toluene was most suitable as a diluent for the five DPAHs system due to good solubility and extraction effect. The influence of acidity (pH) and ligand concentration on the extraction of Am^{3+} and Eu^{3+} was investigated.

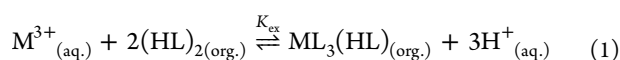
Figure 2 shows the pH effect. It is clear that both D_{Am} and D_{Eu} increase with the increase of pH value. The linear regression between $\log D$ and pH gave slope values close to 3 for all the five extraction systems, implying a cation-exchange extraction model in which three protons are exchanged to the aqueous phase for the extraction of each metal. As is well-known, the pH at which 50% of the metal ion is extracted can be defined as the $pH_{1/2}$ value and can be used as an indication of the extractability of a given ligand. Lower $pH_{1/2}$ value means stronger extractability. The data listed in Table 1 show that the

Table 1. $pH_{1/2}$ Values of the Five DPAH Ligands and Cyanex 301

ligands	$pH_{1/2}$	
	Am^{3+}	Eu^{3+}
HL _I	2.63	2.99
HL _{II}	1.95	2.79
HL _{III}	3.29	4.21
HL _{IV}	2.43	2.92
HL _V	1.57	2.73
Cyanex 301	3.16 ⁴⁷	4.42 ⁴⁷

$pH_{1/2}$ values for both Am^{3+} and Eu^{3+} are in the sequence of $HL_V < HL_{II} < HL_{IV} < HL_I < HL_{III}$, which is in accordance with the order of the pK_a values. Moreover, since DPAHs with the electron-withdrawing group $-CF_3$ are easier to be deprotonated than those with electron-donating groups, they exhibit stronger extractability than the latter.

The stoichiometry of the extracted complex was further determined by the commonly used slope analysis method. The dependence of the distribution ratios (D) of Am^{3+} and Eu^{3+} on the ligand concentrations is shown in Figure 3. To make sure the D values are in a reasonable range for accurate measurement, we adjusted the equilibrium pH of the aqueous phase to 3.50 for HL_V, 2.50 for HL_{II}, 4.00 for HL_{III}, 3.00 for HL_{IV}, and 2.35 for HL_I. As shown in Figure 3, the plots of $(\log D - 3pH)$ vs $\log C_{HL}$ provide straight lines with slope values of about 2 for both Am^{3+} and Eu^{3+} . Because DPAHs are prone to dimerize in nonpolar solvent,¹² the apparent reaction for the extraction of Am^{3+} and Eu^{3+} by the five ligands in toluene can be described as eq 1:



where K_{ex} represents the equilibrium constants for the reaction and can be defined as

$$K_{ex} = \frac{[ML_3(HL)]_{(org.)} \times [H^+]^3_{(aq.)}}{[M^{3+}]_{(aq.)} \times [(HL)_2]_{(org.)}^2} \quad (2)$$

Rearranging and taking the logarithm of eq 2, K_{ex} can be further expressed as

$$\log K_{ex} = \log D - 3pH_{(aq.)} - 2\log[(HL)_2]_{(org.)} + \log Y \quad (3)$$

where $Y = 1 + \beta_1[NO_3^-] + \beta_2[NO_3^-]^2$. β_1 and β_2 are the overall stability constants for the first and second nitrate complexes of M^{3+} , respectively. The Y values have been reported in the literature⁴⁸ and are 3.20 for Am^{3+} and 3.42 for Eu^{3+} . The K_{ex} values were then calculated and the results are listed in Table S2 in the Supporting Information.

Moreover, the $SF_{Am/Eu}$ values under different ligand concentrations can be calculated through the D values, and the results are listed in Table 2. It can be seen that the $SF_{Am/Eu}$ values decrease in the order of $HL_V > HL_{III} > HL_{II} > HL_{IV} > HL_I$, which is different from the sequence of D values. Generally, there is no exact correlation between extractability and selectivity. The higher $SF_{Am/Eu}$ values of HL_V, HL_{III}, and HL_{II} than that of HL_{IV} and HL_I might be ascribed to both electronic and steric effects of the substituent groups, which requires further exploration in the future. The above extraction experiments show that HL_V exhibits the best performance not only on the extractability but also on the selectivity among the five ligands.

Complexation. To better understand the above-mentioned extraction model, the complexation behavior of Eu^{3+} with DPAHs was investigated. In consideration of the high radioactivity of $^{241}Am^{3+}$, only the stable Eu^{3+} was studied in this work. In the extraction system, not only will the DPAH ligand be involved in the complexation with Eu^{3+} , H_2O or NO_3^- might also coordinate with Eu^{3+} because of the high coordination number of Eu^{3+} .^{9,49,50} Thus, luminescence spectroscopy, Raman spectroscopy, and ESI-MS were carried out to illustrate the composition and coordination mode of the Eu-DPAH complexes.

Luminescence Spectroscopy Analysis. The representative luminescence emission spectra of Eu^{3+}/HL_V are shown in Figure 4a. The three emission bands around 594, 618, and 698 nm are attributed to the ${}^5D_0-{}^7F_1$, ${}^5D_0-{}^7F_2$, and ${}^5D_0-{}^7F_4$ transitions of Eu^{3+} , respectively.^{51,52} Considerable decrease of the emission intensity was observed as the mole ratio of C_{HLV}/C_{Eu} approached 4.0. The decrease of the emission intensity can be probably ascribed to the luminescence quenching effect of the $-SH$ group of DPAH when Eu^{3+} was complexed with the ligands during the titration. When the mole ratio of C_{HLV}/C_{Eu} further increased, the spectra only show small changes, which means few new complexes formed afterward. Similar phenomenon can also be observed in other systems, which are summarized in Figure S8a–h in the Supporting Information.

For Eu^{3+} ion, the ${}^5D_0-{}^7F_1$ transition is magnetic-dipole allowed and insensitive to the ligand field. In contrast, the ${}^5D_0-{}^7F_{2,3,4}$ transitions are electric-dipole allowed, and they are hypersensitive to the coordination environment.^{53,54} Accordingly, the local environment of Eu^{3+} can be qualified by the asymmetry factor (AF) through eq 4:

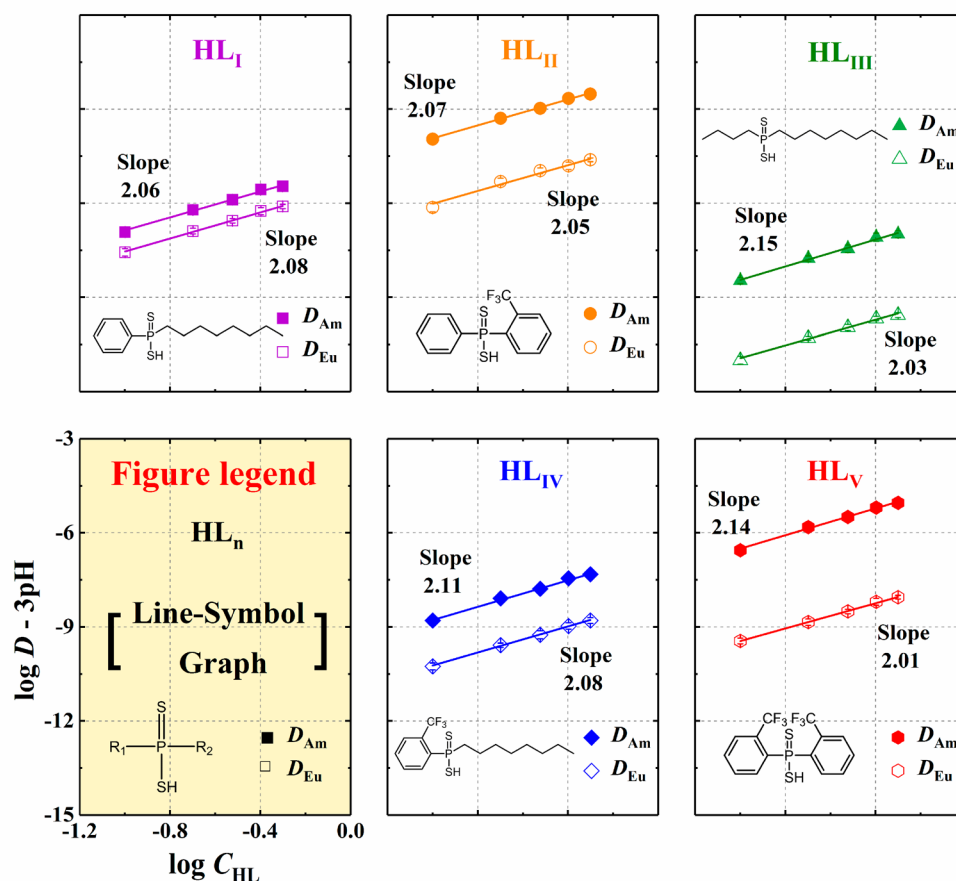


Figure 3. Influence of the ligand concentration on the distribution ratios of Am^{3+} and Eu^{3+} . Organic phase: different concentrations of ligands in toluene. Aqueous phase: trace amount of $^{241}\text{Am}^{3+}$ and/or 200 ppm Eu^{3+} and 1.0 mol/L NaNO_3 in HNO_3 solution with pH 3.50, 2.50, 4.00, 3.00, and 2.35 for HL_I , HL_{II} , HL_{III} , HL_{IV} , and HL_V , respectively. Temperature: 25.0 ± 0.5 °C.

Table 2. $SF_{\text{Am/Eu}}$ Values of the Five Ligands

ligands	$SF_{\text{Am/Eu}}$				
	$C_{\text{HL}} \text{ (mol/L)}$				
	0.10	0.20	0.30	0.40	0.50
HL_I	4.2 ± 0.3	4.9 ± 0.5	4.7 ± 0.4	4.8 ± 0.5	4.4 ± 0.4
HL_{II}	175 ± 16	107 ± 11	97 ± 9	143 ± 12	126 ± 12
HL_{III}	340 ± 34	327 ± 33	318 ± 32	390 ± 30	377 ± 36
HL_{IV}	29 ± 2.4	31 ± 2.7	29 ± 2.3	33 ± 3.1	30 ± 3.2
HL_V	775 ± 73	1062 ± 97	1029 ± 90	1014 ± 102	1020 ± 98

$$AF = I(^5D_0 - ^7F_2) / I(^5D_0 - ^7F_1) \quad (4)$$

where $I(^5D_0 - ^7F_2)$ and $I(^5D_0 - ^7F_1)$ are the intensities of $^5D_0 - ^7F_2$ (~ 617 nm) and $^5D_0 - ^7F_1$ (~ 594 nm) transitions, respectively. As shown in Figure 4b, with the increase of $\text{HL}_V/\text{Eu}^{3+}$ ratio, the AF values decrease gradually and become relatively constant after $C_{\text{HL}_V}/C_{\text{Eu}} = 4.0$, which is similar to the trend of the change of the emission intensity. The AF values of Eu^{3+} complexes with the five ligands at several representative $C_{\text{HL}}/C_{\text{Eu}}$ ratios are listed in Table 3. It can be seen that the difference between $AF_{0.0}$ and $AF_{4.0}$ values decreases in the sequence of $\text{HL}_V > \text{HL}_{II} > \text{HL}_{IV} > \text{HL}_I > \text{HL}_{III}$, which is in agreement with the order of extractability.

The complexation of Eu^{3+} with the five DPAHs was also examined by luminescence lifetime measurements. As shown in Figure 5, the decay lifetime of “free” Eu^{3+} increases obviously upon complexation with DPAHs. All of the

luminescence decay curves of the five Eu -DPAH complexes follow a monoexponential pattern, indicating the presence of a single species. The lifetimes of Eu^{3+} and the coordination species are summarized in Table S4 in the Supporting Information. In the cases where nonradiative processes other than the coupling with $-\text{OH}$ and vibrations are absent or negligible, the number of $-\text{OH}$ groups (N_{OH}) in the inner-sphere can be calculated by eq 5:^{52,55–57}

$$N_{\text{OH}} = 2 \times (1.05/\tau) - 0.44 \quad (5)$$

where τ represents the decay lifetime. Substituting the lifetime into eq 5, the N_{OH} value was calculated to be about 2 for all the complexes, indicating the presence of 1 H_2O molecule or 2 EtOH molecules in the primary coordination sphere of Eu^{3+} in the complexes. It should be noted that in the present Eu -DPAH complexation system, the DPAH ligand is also likely to quench the luminescence of Eu^{3+} as indicated by the titration

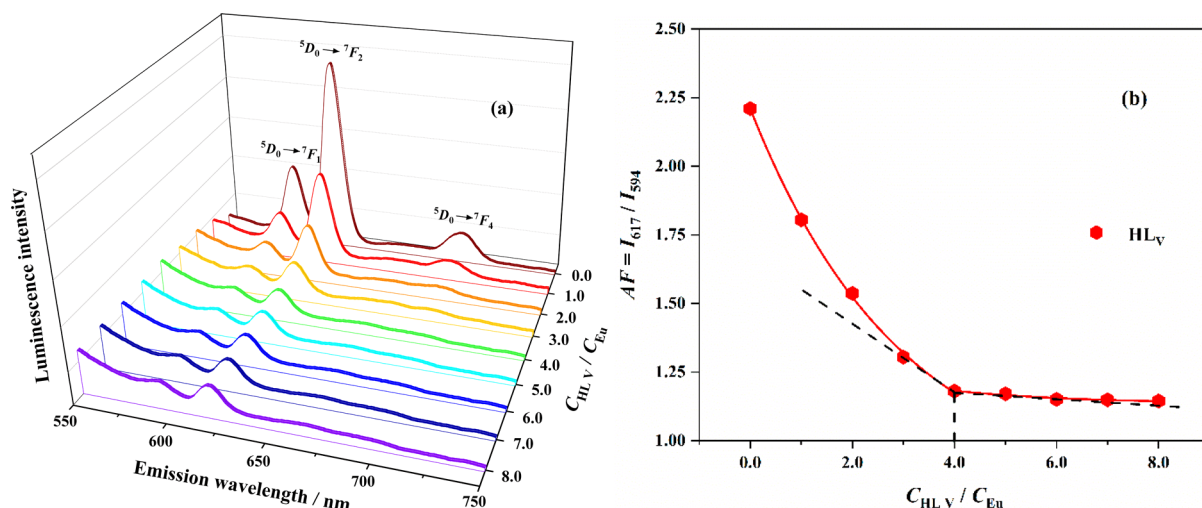


Figure 4. Luminescence titration of $\text{Eu}(\text{NO}_3)_3 \cdot 6\text{H}_2\text{O}$ with HL_V . Luminescence emission spectra (a) and AF values (b) at different $C_{\text{HL}_V}/C_{\text{Eu}}$ ratios. Initial solution: $[\text{Eu}(\text{NO}_3)_3 \cdot 6\text{H}_2\text{O}] = 1.0 \text{ mmol/L}$, volume = 2.0 mL. Titrant: [ligand] = 50 mmol/L. Excitation wavelength: 394 nm. Solvent: EtOH/ H_2O (99/1%, v/v).

Table 3. AF Values at Different $C_{\text{HL}}/C_{\text{Eu}}$ Ratios

ligands	AF values					ΔAF values $ AF_{0,0} - AF_{4,0} $
	$C_{\text{HL}}/C_{\text{Eu}}$ ratios					
	0.0	1.0	2.0	3.0	4.0	
HL_I	2.20	1.91	1.75	1.57	1.42	0.78
HL_{II}	2.20	1.76	1.56	1.41	1.32	0.88
HL_{III}	2.20	2.11	2.04	1.97	1.91	0.29
HL_{IV}	2.21	1.86	1.61	1.46	1.36	0.85
HL_V	2.21	1.80	1.54	1.30	1.18	1.03

results in Figure 4a, and such an effect should not be ignored to analyze the lifetime results. Therefore, the number of the $-\text{OH}$ groups in the Eu-DPAH complexes calculated by eq 5 can only be taken for reference. More accurate correlation between the lifetime and the coordination number of S and $-\text{OH}$ in the complexes is required to be established in future work.

Raman Spectroscopy Analysis. Raman spectroscopy can provide additional information on the coordination environment of the Eu-DPAH complexes, especially it can be used to determine whether or not NO_3^- participates in the coordination with Eu^{3+} . The Raman spectra of $\text{Eu}(\text{NO}_3)_3$ and the Eu-DPAH complexes are shown in Figure 6. It can be seen obviously that the Raman spectra of the Eu-DPAH complexes show basically the same pattern and are very different from that of $\text{Eu}(\text{NO}_3)_3$. The sharp peak at 1515 cm^{-1} in $\text{Eu}(\text{NO}_3)_3$ spectrum can be assigned to NO_3^- . Since such a characteristic peak of NO_3^- was not observed in the spectra of Eu-DPAH complexes, NO_3^- should be absent in the Eu-DPAH complexes.

ESI-MS Analysis. To further identify the extracted species, ESI-MS analysis of the ligands and the Eu-loaded organic phases after extraction was carried out. Figure 7a shows the representative mass spectrum (in positive mode) of HL_V before extraction. An obvious peak appeared at $m/z = 772.9641$, and it can be assigned to $[2(\text{HL}_V) + \text{H}]^+$, indicating

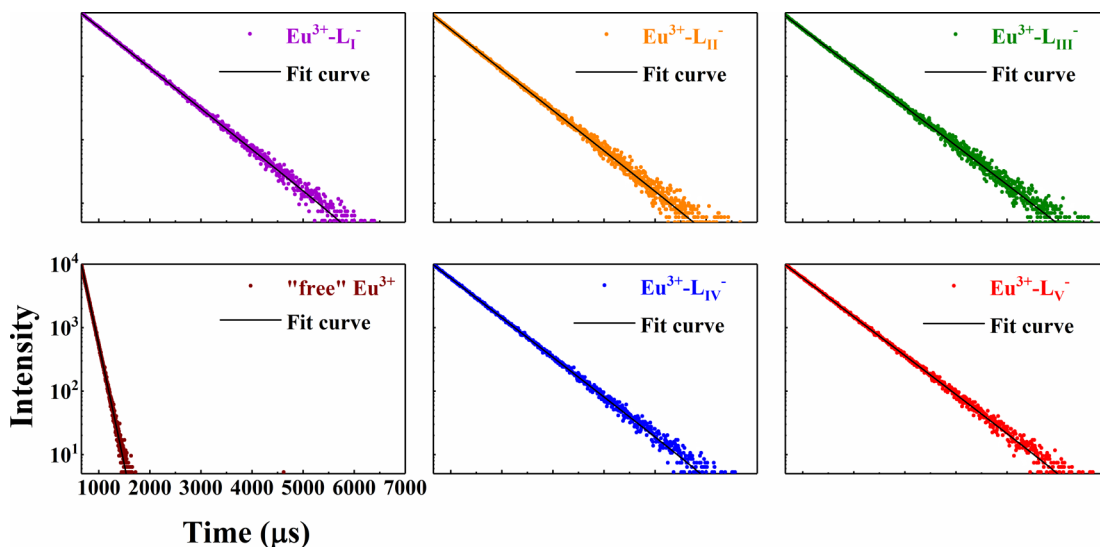


Figure 5. Luminescence decay of "free" Eu^{3+} and the Eu-DPAH complexes.

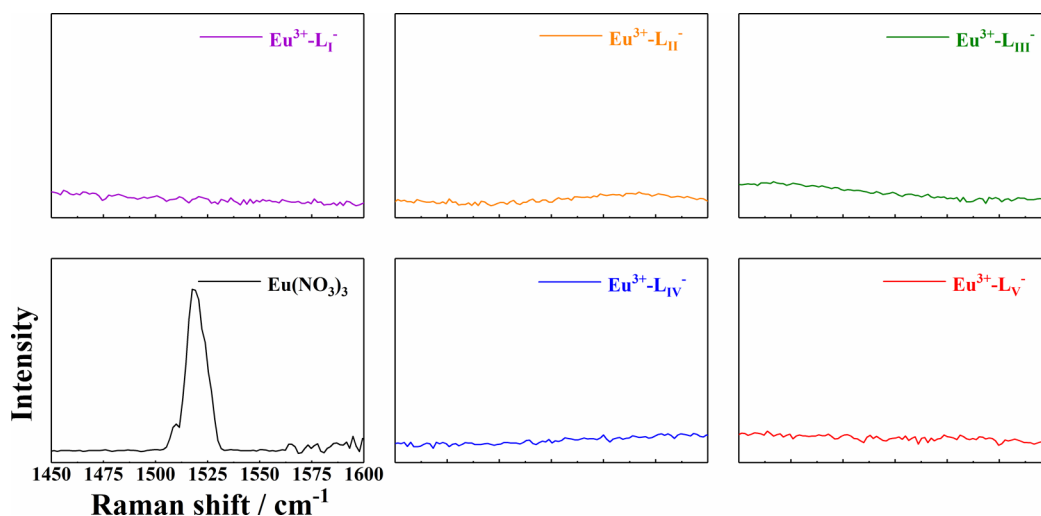


Figure 6. Raman spectra of $\text{Eu}(\text{NO}_3)_3$ and the Eu-DPAH complexes.

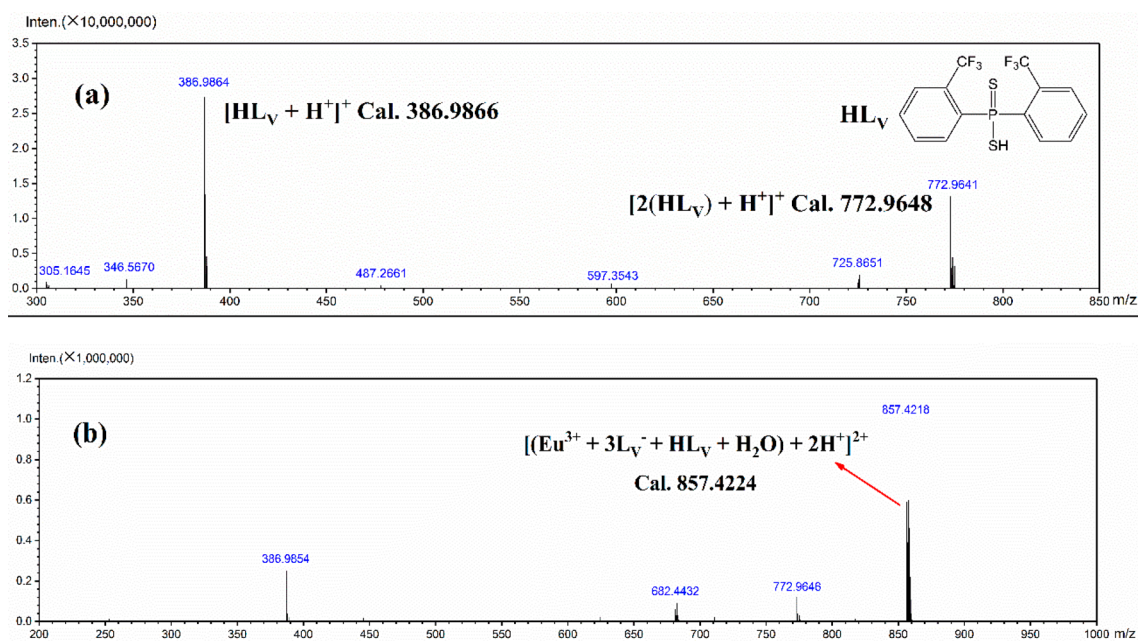


Figure 7. ESI-MS spectra of 0.5 mol/L HL_v in toluene before extraction (a) and the Eu-loaded organic phase after extraction (b).

that DPAH ligands undergo dimerization in the nonpolar or low-polar solvent. Similar results are also observed for the other four ligands (Figure S9 in the Supporting Information). Meanwhile, a prominent peak at $m/z = 386.9864$ can be assigned to $[\text{HL}_v + \text{H}^+]^+$, indicating that the dimer molecule $(\text{HL})_2$ with weak intermolecular interaction is easily discretized to monomers in the process of mass measurement.⁵⁸

The spectrum of the Eu-loaded organic phase after extraction is shown in Figure 7b. According to the results obtained from the aforementioned extraction and complexation studies, DPAH ligand can form 4:1 type complex with Eu^{3+} accompanied by H_2O or EtOH molecules in the inner coordination sphere of Eu^{3+} . Since there is no EtOH molecule involved in the extraction process, the maximum peak at $m/z = 857.4218$ can be assigned to $[(\text{Eu}^{3+} + 3\text{L}_v^- + \text{HL}_v + \text{H}_2\text{O}) + 2\text{H}^+]^{2+}$, which is also confirmed by isotope simulated calculations ($m/z = 857.4224$). Besides, the small peaks at $m/z = 386.9854$, 682.4432 , and 772.9646 can be assigned to

$[\text{HL}_v + \text{H}^+]^+$, $[(\text{Eu}^{3+} + 3\text{L}_v^- + 3\text{H}_2\text{O}) + 2\text{H}^+]^{2+}$, and $[2(\text{HL}_v) + \text{H}^+]^+$, respectively. The ESI-MS results of the other four Eu-loaded organic phases (Figure S9 in the Supporting Information) also suggest that DPAH molecules can coordinate with Eu^{3+} at a mole ratio of 4:1.

DFT Calculations. The above experimental results show that the extraction behaviors of the five ligands are closely relevant to their structures. Herein, DFT calculations have been carried out to further reveal the coordination behavior of Eu^{3+} and Am^{3+} with DPAH ligands. We must note here that the optimized structures of the extracted species $\text{AmL}_3(\text{HL})\text{-(H}_2\text{O)}$ cannot be obtained by the traditional B3LYP functional due to the lack of dispersion corrections. Meanwhile, since the C_6 coefficients or covalent radius R_{cov} for americium element ($\text{IA} = 95$) is not included in the dispersion-correction DFT method (DFT-D), so the corresponding functional such as $\omega\text{B97X-D}$, PBE0-D3 , and B3LYP-D3 also cannot be used for the calculations of Am^{3+} complexes. Our detailed studies

suggest that such a problem could be well-solved by the Minnesota new functional M06-2X that includes a “dispersion-like effect”.⁵⁹ Besides, methyl was used to substitute the more complicated alkyl/aryl groups in the DPAH ligands so as to improve the calculation efficiency.

Extraction Reaction Energies. First, the binding energies of Eu^{3+} with the simplified DPAH ligand were calculated. The results are listed in Table S5 in the Supporting Information and further confirm the formation of the $\text{EuL}_3(\text{HL})(\text{H}_2\text{O})$ complex. On the basis of the extraction results in this work, similar extraction models were found for Am^{3+} and Eu^{3+} during the biphasic equilibrium. Accordingly, we speculate that similar Am^{3+} species might form in the complexation with DPAH ligands. To reveal the coordination mode between DPAH and Am^{3+} , calculations on the changes in Gibbs free energies (ΔG , $\text{kJ}\cdot\text{mol}^{-1}$) for the extraction of hydrated $\text{Am}^{3+}/\text{Eu}^{3+}$ ions ($[\text{M}(\text{H}_2\text{O})_9]^{3+}$) by DPAHs were performed. Herein, NO_3^- was not included in the hydrated metal ion due to its weak coordination with the metal ion in aqueous solutions.

As listed in Table 4, the ΔG of the extraction reaction $[\text{Am}(\text{H}_2\text{O})_9]^{3+} \rightarrow \text{AmL}_3(\text{HL})$ and $[\text{Am}(\text{H}_2\text{O})_9]^{3+} \rightarrow$

Table 4. Calculated Changes in Gibbs Free Energies (ΔG , $\text{kJ}\cdot\text{mol}^{-1}$) for the Extraction of Hydrated $\text{Am}^{3+}/\text{Eu}^{3+}$ Ions ($[\text{M}(\text{H}_2\text{O})_9]^{3+}$) by DPAH using the DFT/M06-2X Method

reaction	ΔG (M = Eu)	ΔG (M = Am)
$[\text{M}(\text{H}_2\text{O})_9]^{3+} \rightarrow \text{ML}_3(\text{HL})$	–	–69.5
$[\text{M}(\text{H}_2\text{O})_9]^{3+} \rightarrow \text{ML}_3(\text{HL})(\text{H}_2\text{O})$	–34.3	–67.4

$\text{AmL}_3(\text{HL})(\text{H}_2\text{O})$ was calculated to be $-69.5 \text{ kJ}\cdot\text{mol}^{-1}$ and $-67.4 \text{ kJ}\cdot\text{mol}^{-1}$, respectively, suggesting that both of these reactions are spontaneous. According to Tian's work, the molecular formula of the Am^{3+} complex was deduced as HAmL_4 , in which no inner-sphere coordinated water is present.^{20,21} Nevertheless, our theoretical calculations suggest that there is no apparent difference on the ΔG values between $\text{AmL}_3(\text{HL})$ and $\text{AmL}_3(\text{HL})(\text{H}_2\text{O})$. Therefore, we suppose that both of these two species are likely to be present in the extraction of Am^{3+} by DPAHs. On the other hand, the ΔG value for $[\text{Eu}(\text{H}_2\text{O})_9]^{3+} \rightarrow \text{EuL}_3(\text{HL})(\text{H}_2\text{O})$ is $-34.3 \text{ kJ}\cdot\text{mol}^{-1}$, which is much less negative than that of the proposed Am^{3+} species. The striking difference on ΔG values may be one

of the reasons for the excellent selectivity to Am^{3+} over Eu^{3+} by DPAH ligands. Figure 8 shows the optimized structures of the stationary points for $\text{EuL}_3(\text{HL})(\text{H}_2\text{O})$, $\text{AmL}_3(\text{HL})$ and $\text{AmL}_3(\text{HL})(\text{H}_2\text{O})$ complexes as well as some key bond lengths (in angstroms).

Molecular Orbitals Analysis for Metal-Sulfur Complexing Bonds. To understand the selectivity to Am^{3+} over Eu^{3+} by DPAHs from the viewpoint of electronic structure, the molecular orbitals and the orbital composition for the $\text{ML}_3(\text{HL})(\text{H}_2\text{O})$ (M = Am or Eu) complexes were analyzed, and the results are shown in Figure 9. The characteristic

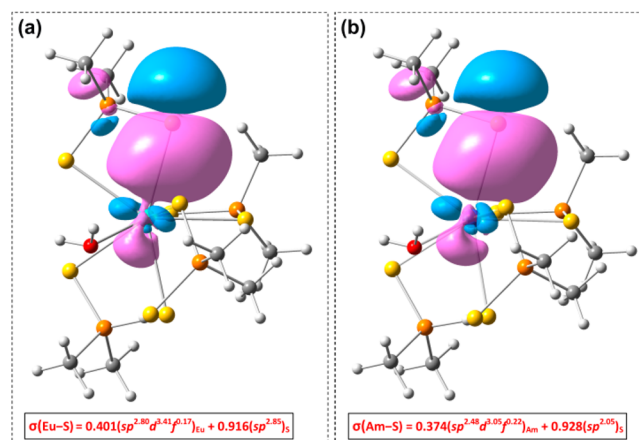


Figure 9. Molecular orbitals and their composition (α -spin state) for (a) Eu–S bond in $\text{EuL}_3(\text{HL})(\text{H}_2\text{O})$ complex and (b) Am–S bond in $\text{AmL}_3(\text{HL})(\text{H}_2\text{O})$ complex.

annuluses of f-orbitals are obvious in Eu–S and Am–S bond molecular orbitals. The $\sigma(\text{M}-\text{S})$ bond molecular orbital composition analysis reveals that the Eu–S and Am–S bonds are in essence the interaction between the unoccupied valence orbitals of Eu^{3+} and Am^{3+} ion (especially 4f and 5d orbitals for Eu^{3+} ; 5f and 6d orbitals for Am^{3+}) and the strong electron-donating sulfur lone pair (sp^3 -hybridized orbitals).⁶⁰ As shown in Table 5, the change in f-orbital occupancy numbers $\Delta N([\text{M}(\text{H}_2\text{O})_9]^{3+} \rightarrow \text{ML}_3(\text{HL})(\text{H}_2\text{O}))$ of Am^{3+} is 0.050, and it is larger than that of Eu^{3+} (0.028), which suggests that the 5f orbital of Am^{3+} has stronger interaction with sp^3 -hybridized orbital of S atom in DPAH ligand than the 4f

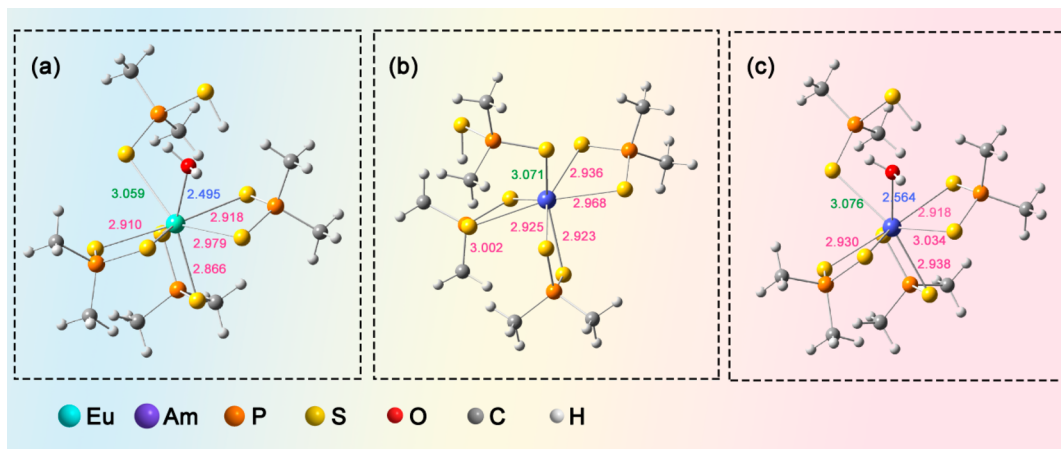


Figure 8. Optimized structures of the stationary points for the complex (a) $\text{EuL}_3(\text{HL})(\text{H}_2\text{O})$, (b) $\text{AmL}_3(\text{HL})$, and (c) $\text{AmL}_3(\text{HL})(\text{H}_2\text{O})$ obtained by the DFT/M06-2X method.

Table 5. Natural f-Orbital Occupancy Numbers (N_f) of Eu and Am in the Complexes, Change in Occupancy Numbers ΔN_f ($[\text{M}(\text{H}_2\text{O})_9]^{3+} \rightarrow \text{ML}_3(\text{HL})(\text{H}_2\text{O})$), Mulliken Spin Density of Eu and Am (D_S), and Change in Spin Density ΔD_S ($[\text{M}(\text{H}_2\text{O})_9]^{3+} \rightarrow \text{ML}_3(\text{HL})(\text{H}_2\text{O})$)

species	N_f	ΔN_f	D_S	ΔD_S
$[\text{Eu}(\text{H}_2\text{O})_9]^{3+}$	6.018	0.028	6.057	0.098
$\text{EuL}_3(\text{HL})(\text{H}_2\text{O})$	6.046		6.155	
$[\text{Am}(\text{H}_2\text{O})_9]^{3+}$	6.055	0.050	6.052	0.141
$\text{AmL}_3(\text{HL})(\text{H}_2\text{O})$	6.105		6.193	

orbital of Eu^{3+} . In addition, the change in spin density $\Delta D_S([\text{Eu}(\text{H}_2\text{O})_9]^{3+} \rightarrow \text{EuL}_3(\text{HL})(\text{H}_2\text{O}))$ in Eu^{3+} complex is 0.098, and it is smaller than that in Am^{3+} complex (0.141), which further indicates that the unoccupied valence orbitals of Am^{3+} display a stronger affinity to the sulfur lone pair than those of Eu^{3+} . These results agree well with the calculated extraction reaction energies listed in Table 4.

The natural atomic orbital occupancies of Eu^{3+} and Am^{3+} valence shell are shown in Table S6 in the Supporting Information. Both the f orbital occupancies and the d orbital occupancies of metal ion in $[\text{M}(\text{H}_2\text{O})_9]^{3+}$ ($\text{M} = \text{Am}$ or Eu) are found to be lower than those in $\text{ML}_3(\text{HL})(\text{H}_2\text{O})$, indicating that the DPAH ligand possesses stronger coordination ability to $\text{Eu}^{3+}/\text{Am}^{3+}$ ions than water molecules. The increase of orbital occupancies after complexation can be attributed to the filling of lone pair electrons of S. Besides, much greater changes of d orbitals than that of f orbitals indicate that the former is more sensitive to the coordination environment than the latter. The natural charges of Eu and Am (q_M) decrease from 1.702 to 0.237 and 1.772 to 0.343, respectively, before and after complexation, which can be attributed to the dispersion by the coordinated S atom. Moreover, it is clear that the WBI between the metal and the ligands ($\text{WBI}(\text{M}-\text{S}_L)$) are significantly larger than those between the metal and H_2O ($\text{WBI}(\text{M}-\text{O}_w)$), which might be resulted from the ligand-exchange reaction. The results show good agreement with the calculated extraction energies (see Table 4).

Deprotonation Parameters and Bond Orders. As mentioned earlier, the extractability of DPAH depends largely on its acidity. To elaborate the extractabilities, the deprotonation processes of $\text{HL}_I - \text{HL}_V$ in aqueous medium were evaluated using M06-2X and B3LYP-D3 hybrid functionals. The corresponding results are summarized in Table 6. As we can see, energy profiles obtained by the two methods show that HL_V possesses the lowest deprotonation energy (ΔE) as compared to other ligands. The trends are also reflected in the

Table 6. Calculated Thermodynamic Parameters (kcal·mol⁻¹) for the Deprotonation of DPAH Ligands in Aqueous Medium (CPCM/UFF) at the Theoretical Levels M06-2X and B3LYP-D3

reaction	M06-2X			B3LYP-D3		
	ΔE	ΔH	ΔG	ΔE	ΔH	ΔG
$\text{HL}_I \rightarrow \text{H}^+ + \text{L}_I^-$	161.6	162.2	155.8	166.9	167.5	161.4
$\text{HL}_{II} \rightarrow \text{H}^+ + \text{L}_{II}^-$	159.5	160.1	153.4	165.3	165.9	158.9
$\text{HL}_{III} \rightarrow \text{H}^+ + \text{L}_{III}^-$	162.6	163.2	157.1	167.9	168.5	161.8
$\text{HL}_{IV} \rightarrow \text{H}^+ + \text{L}_{IV}^-$	160.8	161.4	155.7	166.3	166.8	161.0
$\text{HL}_V \rightarrow \text{H}^+ + \text{L}_V^-$	158.5	159.1	152.1	164.3	164.9	158.2

order of ΔH and ΔG values. It is clear that all the thermodynamic parameters, including ΔE , ΔH , and ΔG values, increase in the order of $\text{HL}_V < \text{HL}_{II} < \text{HL}_{IV} < \text{HL}_I < \text{HL}_{III}$, which is opposite to the sequence of extractability. As aforementioned, the stronger extraction ability of DPAHs to the trivalent metal ion is usually associated with lower deprotonation energy. Therefore, the results from DFT calculations fully support the conclusions of extraction experiments.

Apart from the thermodynamic parameters, the WBI of S–H bond on different DPAH ligands and the nature charges (Q) of sulfur atom on different ligands after deprotonation are also analyzed at the same theoretical levels. As shown in Table 7,

Table 7. WBI of S–H bond in Different DPAH Ligands and Nature Charges (Q) of Sulfur Atom in Different Deprotonated Ligands Obtained by NBO Analysis at the Theoretical Levels M06-2X and B3LYP-D3

ligands	WBI(S–H)		$Q(\text{S})$	
	M06-2X	B3LYP	M06-2X	B3LYP
HL_I	0.945	0.946	−0.790	−0.795
HL_{II}	0.942	0.942	−0.745	−0.748
HL_{III}	0.946	0.948	−0.818	−0.823
HL_{IV}	0.944	0.945	−0.774	−0.776
HL_V	0.940	0.941	−0.724	−0.722

the order of WBI values for S–H bond is $\text{HL}_V < \text{HL}_{II} < \text{HL}_{IV} < \text{HL}_I < \text{HL}_{III}$. Meanwhile, the order of absolute nature charges (Q) of sulfur atom after deprotonation is $\text{L}_V^- < \text{L}_{II}^- < \text{L}_{IV}^- < \text{L}_I^- < \text{L}_{III}^-$, which is consistent with the order of WBI values as well as the sequence of deprotonation energy in Table 6. These results show good agreement with the order of extractability of the five ligands.

CONCLUSIONS

Five DPAH ligands bearing dialkyl, diaryl, or alkyl-aryl substituted groups were synthesized, and their extraction behavior toward Am^{3+} and Eu^{3+} as well as the complexation behavior with Eu^{3+} were investigated. The extractability and selectivity to Am^{3+} over Eu^{3+} by these ligands were also elucidated by DFT calculations. The DPAH ligands containing electron-withdrawing group $-\text{CF}_3$ have shown stronger extractability. Slope analysis suggests that Am^{3+} and Eu^{3+} were extracted as the 4:1 type (ligand:metal) species into the organic phase (toluene). Luminescence, Raman, and ESI-MS analyses indicate that $\text{EuL}_3(\text{HL})(\text{H}_2\text{O})$ was the dominant Eu complex for all the five DPAH ligands. Further DFT calculations illustrate that the protonation property of the ligands is closely related to the extractability. Moreover, molecular orbital analysis indicates that the stronger covalence in $\text{Am}-\text{S}$ bond as compared to that of $\text{Eu}-\text{S}$ bond is a key factor for the excellent selectivity to Am^{3+} over Eu^{3+} by DPAH ligands. Although the studied five ligands are insufficient to represent all DPAHs, the results from this work could help us better understand the relevant extraction and complexation model at the molecular level and also provide valuable experimental and theoretical guidance for designing more efficient S-donor ligands for $\text{An}^{3+}/\text{Ln}^{3+}$ separation in the future.

■ ASSOCIATED CONTENT

S Supporting Information

The Supporting Information is available free of charge on the ACS Publications website at DOI: 10.1021/acs.inorgchem.8b01635.

Additional experimental details and data (PDF)

■ AUTHOR INFORMATION

Corresponding Authors

*E-mail: dsd68@163.com.

*E-mail: xuchao@tsinghua.edu.cn.

*E-mail: typhysics@163.com.

ORCID 

Chao Xu: 0000-0001-5539-4754

Songdong Ding: 0000-0003-4949-3080

Author Contributions

^{||}These authors contributed equally to this work.

Notes

The authors declare no competing financial interest.

■ ACKNOWLEDGMENTS

The authors are grateful for the financial support by the National Science Foundation of China (grant nos. 91426302, 11675115, and 91126016). The calculations were performed using supercomputers at Tsinghua National Laboratory for Information Science and Technology. Comprehensive training platform of specialized laboratory (College of chemistry, Sichuan University) is acknowledged for NMR, IR, MS, and ICP-AES analyses. Analytical & Testing Center of Sichuan University is highly acknowledged for providing the analysis of Raman spectra.

■ REFERENCES

- (1) Muller, J. M.; Galley, S. S.; Albrecht-Schmitt, T. E.; Nash, K. L. Characterization of lanthanide complexes with bis-1,2,3-triazole-bipyridine ligands involved in actinide/lanthanide separation. *Inorg. Chem.* **2016**, *55*, 11454–11461.
- (2) Lan, J. H.; Shi, W. Q.; Yuan, L. Y.; Zhao, Y. L.; Li, J.; Chai, Z. F. Trivalent actinide and lanthanide separations by tetradentate nitrogen ligands: a quantum chemistry study. *Inorg. Chem.* **2011**, *50*, 9230–9237.
- (3) Wang, Z. P.; Wang, J. R.; Ding, S. D.; Liu, Y.; Zhang, L. R.; Song, L. J.; Chen, Z. L.; Yang, X. Y.; Wang, X. Y. Non-heterocyclic N-donor ligands of nitrilotriacetamide for Am³⁺/Eu³⁺ separation. *Sep. Purif. Technol.* **2019**, *210*, 107–116.
- (4) Wang, Z. P.; Ding, S. D.; Hu, X. Y.; Li, S. M.; Su, D. P.; Zhang, L. R.; Liu, Y.; Jin, Y. D. Selective extraction of americium(III) over europium(III) ions in nitric acid solution by NTAamide(C8) using a novel water-soluble bisdiglycolamide as a masking agent. *Sep. Purif. Technol.* **2017**, *181*, 148–158.
- (5) Dam, H. H.; Reinhoudt, D. N.; Verboom, W. Multicoordinate ligands for actinide/lanthanide separations. *Chem. Soc. Rev.* **2007**, *36*, 367–377.
- (6) Liu, Y.; Yang, X. Y.; Ding, S. D.; Wang, Z. P.; Zhang, L. R.; Song, L. J.; Chen, Z. L.; Wang, X. Y. Highly efficient trivalent americium/europium separation by phenanthroline-derived bis(pyrazole) ligands. *Inorg. Chem.* **2018**, *57*, 5782–5790.
- (7) Kolarik, Z. Complexation and separation of lanthanides(III) and actinides(III) by heterocyclic N-donors in solutions. *Chem. Rev.* **2008**, *108*, 4208–4252.
- (8) Jansone-Popova, S.; Ivanov, A. S.; Bryantsev, V. S.; Sloop, F. V., Jr; Custelcean, R.; Popovs, I.; Dekarske, M. M.; Moyer, B. A. Bis-lactam-1,10-phenanthroline (BLPhen), a new type of preorganized

mixed N,O-donor ligand that separates Am(III) over Eu(III) with exceptionally high efficiency. *Inorg. Chem.* **2017**, *56*, 5911–5917.

(9) Lewis, F. W.; Harwood, L. M.; Hudson, M. J.; Drew, M. G. B.; Desreux, J. F.; Vidick, G.; Bouslimani, N.; Modolo, G.; Wilden, A.; Sypula, M.; Vu, T. H.; Simonin, J. P. Highly efficient separation of actinides from lanthanides by a phenanthroline-derived bis-triazine ligand. *J. Am. Chem. Soc.* **2011**, *133*, 13093–13102.

(10) Lewis, F. W.; Hudson, M. J.; Harwood, L. M. Development of highly selective ligands for separations of actinides from lanthanides in the nuclear fuel cycle. *Synlett* **2011**, *2011*, 2609–2632.

(11) Zhu, Y. J. The separation of americium from light lanthanides by Cyanex 301 extraction. *Radiochim. Acta* **1995**, *68*, 95–98.

(12) Zhu, Y. J.; Chen, J.; Jiao, R. Z. Extraction of Am(III) and Eu(III) from nitrate solution with purified Cyanex 301. *Solvent Extr. Ion Exch.* **1996**, *14*, 61–68.

(13) Chen, J.; Wang, S. W.; Xu, C.; Wang, X. H.; Feng, X. G. Separation of americium from lanthanides by purified Cyanex 301 countercurrent extraction in miniature centrifugal contactors. *Procedia Chem.* **2012**, *7*, 172–177.

(14) Madic, C.; Boullis, B.; Baron, P.; Testard, F.; Hudson, M. J.; Liljenzin, J. O.; Christiansen, B.; Ferrando, M.; Facchini, A.; Geist, A.; Modolo, G.; Espartero, A. G.; De Mendoza, J. Futuristic back-end of the nuclear fuel cycle with the partitioning of minor actinides. *J. Alloys Compd.* **2007**, *444*, 23–27.

(15) Madic, C.; Testard, F.; Hudson, M. J.; Liljenzin, J. O.; Christiansen, B.; Ferrando, M.; Facchini, A.; Geist, A.; Modolo, G.; Gonzalez-Espartero, A.; Mendoza, J. D. *Part New-New Solvent Extraction Processes for Minor Actinides Final Report*; CEA: France, 2004.

(16) Modolo, G.; Seekamp, S. Hydrolysis and radiation stability of the ALINA solvent for actinide(III)/lanthanide(III) separation during the partitioning of minor actinides. *Solvent Extr. Ion Exch.* **2002**, *20*, 195–210.

(17) Tian, G. X.; Zhu, Y. J.; Xu, J. M. Extraction of Am(III) and Ln(III) by dialkyldithiophosphinic acid with different alkyl groups. *Solvent Extr. Ion Exch.* **2001**, *19*, 993–1005.

(18) Modolo, G.; Nabet, S. Thermodynamic study on the synergistic mixture of bis(chlorophenyl)dithiophosphinic acid and tris(2-ethylhexyl)phosphate for separation of actinides(III) from lanthanides(III). *Solvent Extr. Ion Exch.* **2005**, *23*, 359–373.

(19) Peterman, D. R.; Greenhalgh, M. R.; Tillotson, R. D.; Klaehn, J. R.; Harrup, M. K.; Luther, T. A.; Law, J. D. Selective extraction of minor actinides from acidic media using symmetric and asymmetric dithiophosphinic acids. *Sep. Sci. Technol.* **2010**, *45*, 1711–1717.

(20) Tian, G. X.; Zhu, Y. J.; Xu, J. M.; Hu, T. D.; Xie, Y. N. Characterization of extraction complexes of Am(III) with dialkyldithiophosphinic acids by extended X-ray absorption fine structure spectroscopy. *J. Alloys Compd.* **2002**, *334*, 86–91.

(21) Tian, G. X.; Zhu, Y. J.; Xu, J. M.; Zhang, P.; Hu, T. D.; Xie, Y. N.; Zhang, J. Investigation of the extraction complexes of light lanthanides(III) with bis(2,4,4-trimethylpentyl) dithiophosphinic acid by EXAFS, IR, and MS in comparison with the americium(III) complex. *Inorg. Chem.* **2003**, *42*, 735–741.

(22) Jensen, M. P.; Bond, A. H. Comparison of covalency in the complexes of trivalent actinide and lanthanide cations. *J. Am. Chem. Soc.* **2002**, *124*, 9870–9877.

(23) Cao, X. Y.; Heidelberg, D.; Ciupka, J.; Dolg, M. First-principles study of the separation of Am^{III}/Cm^{III} from Eu^{III} with Cyanex301. *Inorg. Chem.* **2010**, *49*, 10307–10315.

(24) Bhattacharyya, A.; Ghanty, T. K.; Mohapatra, P. K.; Manchanda, V. K. Selective americium(III) complexation by dithiophosphinates: a density functional theoretical validation for covalent interactions responsible for unusual separation behavior from trivalent lanthanides. *Inorg. Chem.* **2011**, *50*, 3913–3921.

(25) Daly, S. R.; Keith, J. M.; Batista, E. R.; Boland, K. S.; Clark, D. L.; Kozimor, S. A.; Martin, R. L. Sulfur K-edge X-ray absorption spectroscopy and time-dependent density functional theory of dithiophosphinate extractants: minor actinide selectivity and elec-

tronic structure correlations. *J. Am. Chem. Soc.* **2012**, *134*, 14408–14422.

(26) Wang, F.; Jia, C.; Chen, J. Convenient synthesis of (*o*-CF₃Ph)₂PS₂H and evaluation in selective extraction of actinides over lanthanides. *J. Radioanal. Nucl. Chem.* **2013**, *298*, 531–536.

(27) Zeng, C. X.; Hu, Q. Determination of the polyacid dissociation constants of glycyrrhizic acid. *Indian J. Chem.* **2008**, *47A*, 71–74.

(28) Gillman, G. P. Influence of organic matter and phosphate content on the point of zero charge of variable charge components in oxidic soils. *Aust. J. Soil Res.* **1985**, *23*, 643–646.

(29) Kohn, W.; Sham, L. J. Self-consistent equations including exchange and correlation effects. *Phys. Rev.* **1965**, *140* (4A), A1133–A1138.

(30) Frisch, M. J.; Trucks, G. W.; Schlegel, H. B.; Scuseria, G. E.; Robb, M. A.; Cheeseman, J. R.; Scalmani, G.; Barone, V.; Mennucci, B.; Petersson, G. A.; Nakatsuji, H.; Caricato, M.; Li, X.; Hratchian, H. P.; Izmaylov, A. F.; Bloino, J.; Zheng, G.; Sonnenberg, J. L.; Hada, M.; Ehara, M.; Toyota, K.; Fukuda, R.; Hasegawa, J.; Ishida, M.; Nakajima, T.; Honda, Y.; Kitao, O.; Nakai, H.; Vreven, T.; Montgomery, J. A., Jr.; Peralta, J. E.; Ogliaro, F.; Bearpark, M.; Heyd, J. J.; Brothers, E.; Kudin, K. N.; Staroverov, V. N.; Kobayashi, R.; Normand, J.; Raghavachari, K.; Rendell, A.; Burant, J. C.; Iyengar, S. S.; Tomasi, J.; Cossi, M.; Rega, N.; Millam, J. M.; Klene, M.; Knox, J. E.; Cross, J. B.; Bakken, V.; Adamo, C.; Jaramillo, J.; Gomperts, R.; Stratmann, R. E.; Yazyev, O.; Austin, A. J.; Cammi, R.; Pomelli, C.; Ochterski, J. W.; Martin, R. L.; Morokuma, K.; Zakrzewski, V. G.; Voth, G. A.; Salvador, P.; Dannenberg, J. J.; Dapprich, S.; Daniels, A. D.; Farkas, O.; Foresman, J. B.; Ortiz, J. V.; Cioslowski, J.; Fox, D. J. *Gaussian 09*, Revision D.01; Gaussian, Inc.: Wallingford, CT, 2009.

(31) Zhao, Y.; Truhlar, D. G. The M06 suite of density functionals for main group thermochemistry, thermochemical kinetics, non-covalent interactions, excited states, and transition elements: two new functionals and systematic testing of four M06-class functionals and 12 other functionals. *Theor. Chem. Acc.* **2008**, *120*, 215–241.

(32) Becke, A. D. Density-functional thermochemistry. III. *J. Chem. Phys.* **1993**, *98*, 5648–5652.

(33) Lee, C.; Yang, W.; Parr, R. G. Development of the Colle-Salvetti correlation-energy formula into a functional of the electron density. *Phys. Rev. B: Condens. Matter Mater. Phys.* **1988**, *37*, 785–789.

(34) Grimme, S.; Antony, J.; Ehrlich, S.; Krieg, H. A consistent and accurate ab initio parametrization of density functional dispersion correction (DFT-D) for the 94 elements H–Pu. *J. Chem. Phys.* **2010**, *132*, 154104.

(35) Dolg, M.; Stoll, H.; Preuss, H. Energy-adjusted abinitio pseudopotentials for the rare earth elements. *J. Chem. Phys.* **1989**, *90*, 1730–1734.

(36) Küchle, W.; Dolg, M.; Stoll, H.; Preuss, H. Energy-adjusted pseudopotentials for the actinides. Parameter sets and test calculations for thorium and thorium monoxide. *J. Chem. Phys.* **1994**, *100*, 7535–7542.

(37) Keith, J. M.; Batista, E. R. Theoretical examination of the thermodynamic factors in the selective extraction of Am³⁺ from Eu³⁺ by dithiophosphinic acids. *Inorg. Chem.* **2012**, *51*, 13–15.

(38) Dolg, M.; Cao, X. Y. Relativistic pseudopotentials: their development and scope of applications. *Chem. Rev.* **2012**, *112*, 403–480.

(39) Barone, V.; Cossi, M. Quantum calculation of molecular energies and energy gradients in solution by a conductor solvent model. *J. Phys. Chem. A* **1998**, *102*, 1995–2001.

(40) Rayne, S.; Forest, K. Theoretical studies on the pK_a values of perfluoroalkyl carboxylic acids. *J. Mol. Struct.: THEOCHEM* **2010**, *949*, 60–69.

(41) Wiberg, K. B. Application of the pople-santry-segal CNDO method to the cyclopropylcarbonyl and cyclobutyl cation and to bicyclobutane. *Tetrahedron* **1968**, *24*, 1083–1096.

(42) Foster, J. P.; Weinhold, F. Natural hybrid orbitals. *J. Am. Chem. Soc.* **1980**, *102*, 7211–7218.

(43) Reed, A. E.; Weinstock, R. B.; Weinhold, F. Natural population analysis. *J. Chem. Phys.* **1985**, *83*, 735–746.

(44) Leavitt, C. M.; Gresham, G. L.; Benson, M. T.; Gaumet, J. J.; Peterman, D. R.; Klaehn, J. R.; Moser, M.; Aubriet, F.; Van Stipdonk, M. J.; Groenewold, G. S. Investigations of acidity and nucleophilicity of diphenyldithiophosphate ligands using theory and gas-phase dissociation reactions. *Inorg. Chem.* **2008**, *47*, 3056–3064.

(45) Perrin, D. D.; Dempsey, B.; Serjeant, E. P. *pK_a prediction for organic acids and bases*; Chapman and Hall: New York, 1981.

(46) Benson, M. T.; Moser, M. L.; Peterman, D. R.; Dinescu, A. Determination of pK_a for dithiophosphinic acids using density functional theory. *J. Mol. Struct.: THEOCHEM* **2008**, *867*, 71–77.

(47) Wang, X. H.; Zhu, Y. J.; Jiao, R. Z. Separation of Am from lanthanides by a synergistic mixture of purified Cyanex 301 and TBP. *J. Radioanal. Nucl. Chem.* **2002**, *251*, 487–492.

(48) Horwitz, E. P.; Muscatello, A. C.; Kalina, D. G.; Kaplan, L. The extraction of selected transplutonium(III) and lanthanide(III) ions by dihexyl-*N*, *N*-diethylcarbamoylmethylphosphonate from aqueous nitrate media. *Sep. Sci. Technol.* **1981**, *16*, 417–437.

(49) Habenschuss, A.; Spedding, F. H. The coordination (hydration) of rare earth ions in aqueous chloride solutions from x-ray diffraction. III. *J. Chem. Phys.* **1980**, *73*, 442–450.

(50) Xiao, C. L.; Wang, C. Z.; Mei, L.; Zhang, X. R.; Wall, N.; Zhao, Y. L.; Chai, Z. F.; Shi, W. Q. Europium, uranyl, and thorium-phenanthroline amide complexes in acetonitrile solution: an ESI-MS and DFT combined investigation. *Dalton Trans.* **2015**, *44*, 14376–14387.

(51) Denecke, M. A.; Rossberg, A.; Panak, P. J.; Weigl, M.; Schimmelpfennig, B.; Geist, A. Characterization and comparison of Cm(III) and Eu(III) complexed with 2,6-di(5,6-dipropyl-1,2,4-triazin-3-yl)pyridine using EXAFS, TRFLS, and quantum-chemical methods. *Inorg. Chem.* **2005**, *44*, 8418–8425.

(52) Weigl, M.; Denecke, M. A.; Panak, P. J.; Geist, A.; Gommer, K. EXAFS and time-resolved laser fluorescence spectroscopy (TRLFS) investigations of the structure of Cm(III)/Eu(III) complexed with di(chlorophenyl)dithiophosphinic acid and different synergistic agents. *Dalton Trans.* **2005**, *7*, 1281–1286.

(53) Sengupta, A.; Wu, L.; Feng, W.; Yuan, L. H.; Natarajan, V. Luminescence investigation on Eu-pillar[5]arene-based diglycolamide (DGA) complexes: nature of the complex, Judd–Ofelt calculations and effect of ligand structure. *J. Lumin.* **2015**, *158*, 356–364.

(54) Zhang, P.; Kimura, T. Complexation of Eu(III) with dibutyl phosphate and tributyl phosphate. *Solvent Extr. Ion Exch.* **2006**, *24*, 149–163.

(55) Choppin, G. R.; Peterman, D. R. Applications of lanthanide luminescence spectroscopy to solution studies of coordination chemistry. *Coord. Chem. Rev.* **1998**, *174*, 283–299.

(56) Kimura, T.; Kato, Y. Luminescence study on hydration states of lanthanide(III)–polyaminopolycarboxylate complexes in aqueous solution. *J. Alloys Compd.* **1998**, *275*, 806–810.

(57) Xu, C.; Sun, T. X.; Rao, L. F. Interactions of bis(2,4,4-trimethylpentyl) dithiophosphinate with trivalent lanthanides in a homogeneous medium: thermodynamics and coordination modes. *Inorg. Chem.* **2017**, *56*, 2556–2565.

(58) Groenewold, G. S.; Peterman, D. R.; Klaehn, J. R.; Delmau, L. H.; Marc, P.; Custelcean, R. Oxidative degradation of bis(2,4,4-trimethylpentyl)dithiophosphinic acid in nitric acid studied by electrospray ionization mass spectrometry. *Rapid Commun. Mass Spectrom.* **2012**, *26*, 2195–2203.

(59) Zhao, Y.; Truhlar, D. G. The M06 suite of density functionals for main group thermochemistry, thermochemical kinetics, non-covalent interactions, excited states, and transition elements: two new functionals and systematic testing of four M06-class functionals and 12 other functionals. *Theor. Chem. Acc.* **2008**, *120*, 215–241.

(60) Otero-Calvi, A.; Montero, L. A.; Stohrer, W. D. DFT modelling of cobalt and nickel complexes with dithiophosphinic acid. *J. Mol. Struct.: THEOCHEM* **2008**, *859*, 93–97.